Molecular Structures of Free–Base Corroles: Nonplanarity, Chirality, and Enantiomerization

4 AUTHORS:

Jan Capar
University of Tromsoe
5 PUBLICATIONS   36 CITATIONS

SEE PROFILE

Jeanet Conradie
University of the Free State
142 PUBLICATIONS   1,833 CITATIONS

SEE PROFILE

Christine M Beavers
Lawrence Berkeley National Laboratory
95 PUBLICATIONS   1,828 CITATIONS

SEE PROFILE

Abhik Ghosh
UiT - The Arctic University of Norway
187 PUBLICATIONS   5,359 CITATIONS

SEE PROFILE

Molecular Structures of Free-Base Corroles: Nonplanarity, Chirality, and Enantiomerization

Jan Capar,[†] Jeanet Conradie,[†,‡] Christine M. Beavers,[§] and Abhik Ghosh*[,†]

[†]Department of Chemistry and Center for Theoretical and Computational Chemistry, University of Tromsø, 9037 Tromsø, Norway
[‡]Department of Chemistry, University of the Free State, 9300 Bloemfontein, Republic of South Africa
[§]Advanced Light Source, Lawrence Berkeley National Laboratory, Berkeley, California 94720, United States

Ⓢ Supporting Information

ABSTRACT: The molecular structures of free-base corroles are illustrative of a variety of bonded and nonbonded interactions including aromaticity, intra- as well as intermolecular hydrogen bonding, steric interactions among multiple NH hydrogens within a congested central cavity, and the effects of peripheral substituents. Against this backdrop, an X-ray structure of 2,3,7,8,12,13,17,18-octabromo-5,10,15-tris-(pentafluorophenyl)corrole, $H_3[Br_8TPFPCor]$, corresponding to a specific tautomer, has been found to exhibit the strongest nonplanar distortions observed to date for any free-base corrole structure. Two adjacent N-protonated pyrrole rings are tilted with respect to each other by approximately 97.7°, while the remainder of the molecule is comparatively planar. Dispersion-corrected DFT calculations were undertaken to investigate to what extent the strong nonplanar distortions can be attributed to steric effects of the peripheral substituents. For *meso*-triphenylcorrole, DFT calculations revealed nonplanar distortions that are only marginally less pronounced than those found for $H_3(Br_8TPFPCor)$. A survey of X-ray structures of sterically unhindered corroles also uncovered additional examples of rather strong nonplanar distortions. Detailed potential energy calculations as a function of different saddling dihedrals also emphasized the softness of the distortions. Because of nonplanar distortions, free-base corrole structures are chiral. For $H_3[Br_8TPFPCor]$, DFT calculations led to an estimate of 15 kcal/mol (0.67 eV) as the activation barrier for enantiomerization of the free-base structures, which is significantly higher than the barrier for NH tautomerism calculated for this molecule, about 5 kcal/mol (0.2 eV). In summary, steric crowding of the internal NH hydrogens appears to provide the main driving force for nonplanar distortions of *meso*-triarylcorroles; the presence of additional β-substituents adds marginally to this impetus.
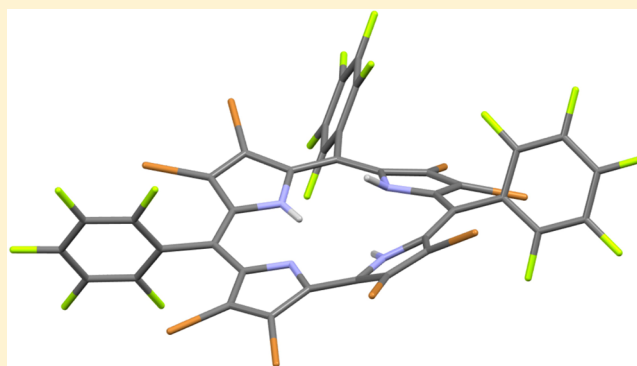
INTRODUCTION

As fully aromatic versions of the corrin ring of B_{12} cofactors, corroles are superficially similar to porphyrins, yet a closer look reveals several important differences. Perhaps the most obvious difference is that free-base porphyrins are diprotic ligands, whereas corroles are triprotic (Figure 1). Corroles also lack one
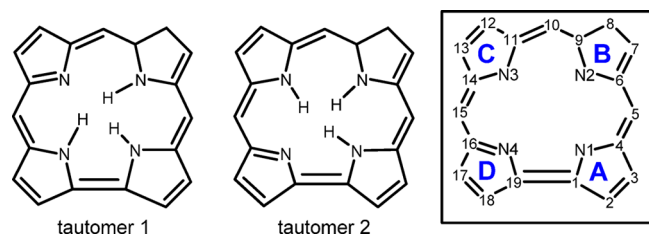
Figure 1. Two possible tautomers of the free base corrole and the numbering scheme used.
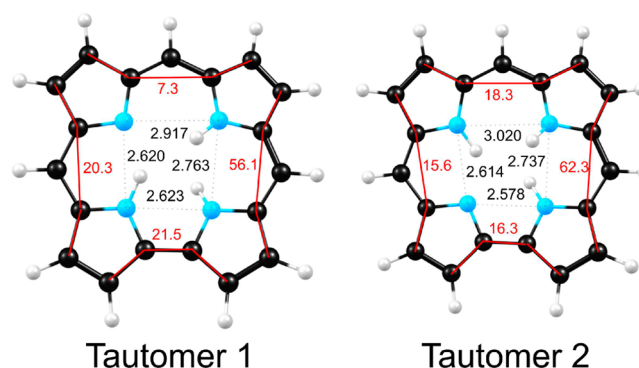

Figure 2. BP86-D/TZP optimized structures of the two tautomers of the unsubstituted free base corrole, $H_3[Cor]$. Distances (Å) are shown in black, and corrole saddling dihedrals, in red (deg). Color code of atoms (online version): C (black), N (blue), H (white).

meso-carbon and their central, metal-binding cavity is accordingly more constricted than that of porphyrins. As tightly binding,

Table 1. Crystal Data for H$_3$[Br$_8$TPFPC]

sample	H$_3$[Br$_8$TPFPC]
chemical formula	C$_{37}$H$_3$N$_4$F$_{15}$Br$_8$· 0.5CH$_2$Cl$_2$
formula mass	1470.18
crystal system	monoclinic
space group	C2/c
λ (Å)	0.6199
a (Å)	21.7652(8)
b (Å)	20.7937(8)
c (Å)	17.9564(7)
α (deg)	90
β (deg)	95.343(2)
γ (deg)	90
Z	8
V (Å^3)	8091.4(5)
temperature (K)	100(2)
density (g/cm^3)	2.414
no. of meased reflections	24 101
no. of unique reflections	17 064
no. of parameters	616
no. of restraints	1
R_{int} (%)	8.18
θ range (deg)	1.184−33.060
R_1, wR_2 all data	0.0700, 0.1416
R_1, wR_2 [$I > 2\sigma(I)$]	0.0452, 0.1235
S (GooF) all data	1.032
max/min res dens (e/Å^3)	+1.694/−1.626

trianionic ligands, corroles give rise to many stable higher-valent transition metal complexes; some of these may be described as noninnocent.[1] Corroles also differ from porphyrins in terms of their conformational properties.[2] Porphyrins are much more susceptible to nonplanar distortions such as ruffling or saddling than corroles. The relative rigidity of corroles vis-à-vis nonplanar distortions may be largely related to the direct C$_1$−C$_{19}$ linkage, which is resistant to both pyramidalization (which would be required for ruffling) and twisting (which would required for saddling). Crystallographic and density functional theory (DFT) studies in our laboratory suggest that whereas ruffling is essentially a forbidden distortion mode for corroles, saddling is largely limited to copper corroles.[3,4] The great majority of metallocorroles are either planar or mildly domed, although a few cases of strong doming are also known.[5]

Against this backdrop, the conformations of free-base corroles are of particular interest. As discussed in more detail below, several X-ray structures of *meso*-triarylcorroles are available and these exhibit significant out-of-plane tilting of one of the N-protonated pyrrole rings. Little exact information, however, is available on sterically encumbered, undecasubstituted free-base corroles. Thus, the central hydrogens of a free-base undecaarylcorrole were found to be disordered.[6] This was also the case in a low-resolution X-ray structure of the important ligand 2,3,7,8,12,13,17,18-octabromo-5,10,15-tris(pentafluorophenyl)-corrole, H$_3$[Br$_8$TPFPCor].[7] Despite the low resolution, the latter structure revealed a dramatically nonplanar corrole macrocycle.
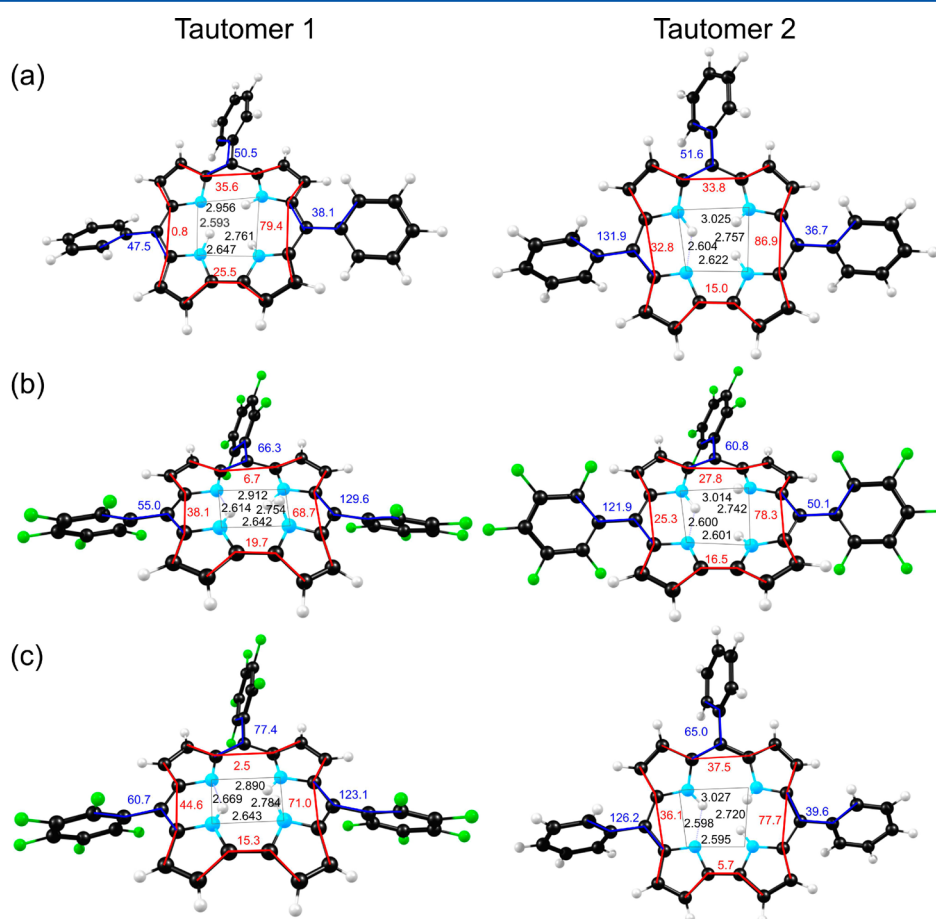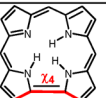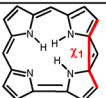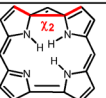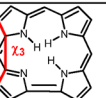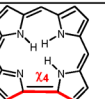

Figure 3. BP86-D/TZP calculated (a) H$_3$[TPCor] and (b) H$_3$[TPFPCor] and (c) experimental structures H$_3$[TPFPCor] (left)[12] and H$_3$[TPCor] (right).[12] Distances (Å) are shown in black, corrole saddling dihedrals in red (deg), and corrole−aryl dihedrals (deg), in blue. Color code of atoms: C (black), N (blue), H (white), F (green).

Table 2. Saddling Dihedrals (deg) for BP86-D/TZP Optimized Structures

	Tautomer 1				Tautomer 2			
	χ_1	χ_2	χ_3	χ_4	χ_1	χ_2	χ_3	χ_4
$H_3[Cor]$	56.1	7.3	30.2	21.5	62.3	18.3	15.6	16.3
$H_3[TPFPCor]$	68.7	6.7	38.1	19.7	78.3	27.8	25.3	16.5
$H_3[TPCor]$	79.4	35.6	0.8	25.5	86.9	33.8	32.8	15.0
$H_3[Br_8TPFPCor]$	85.9	37.8	7.8	39.0	93.8	47.4	14.0	37.4
$H_3[Br_8TPCor]$	100.4	55.5	23.3	44.2	106.3	60.3	25.4	42.2

In this study, we report a high-resolution X-ray structure of $H_3[Br_8TPFPCor]$ that corresponds to a given tautomer (tautomer 2 in the notation of Figure 1).

Encouraged by this successful structure determination, we conducted a thorough DFT study of nonplanar distortion potentials of free-base corroles. One noteworthy point is that the nonplanar conformations of free-base corroles are chiral. Accordingly, we also made an attempt to determine energy barriers associated with enantiomerization. The DFT studies nicely complement the existing experimental data on free-base corroles and shed light on the conformational characteristics of corroles relative to porphyrins.

■ METHODS

Free-base $H_3[Br_8TPFPC]$ was prepared as reported earlier and recrystallized from CH_2Cl_2/n-hexane solution by the slow evaporation technique. A dark green shard of dimensions $0.140 \times 0.080 \times 0.060$ mm^3 was mounted in the 100(2) K nitrogen cold stream provided by a Oxford Cryosystems Cryostream 700 Plus low temperature apparatus on the goniometer head of a Bruker D8 diffractometer equipped with a ApexII CCD detector on beamline 11.3.1 at the Advanced Light Source in Berkeley, CA. Diffraction data were collected using synchrotron radiation monochromated using silicon(111) to a wavelength of 0.6199(1) Å. An approximate full sphere of data to $2\theta_{max} = 67°$ was collected using 0.3° ω scans. The data were integrated using the program SAINT v7.68A. A multiscan correction for absorption was applied using the program SADABS-2008/1. A total of 128 423 reflections were collected, of which 24 101were unique [$R(int) = 0.0818$], and 17 064 were observed [$I > 2\sigma(I)$]. The structure was solved by dual-space methods (SHELXT) and refined by full-matrix least-squares on F^2 (SHELXL-2014) using 616 parameters and one restraint for the disordered solvent. The hydrogen atoms on the pyrrole nitrogens were generated geometrically after careful analysis of the bonding environment, then subsequently allowed to refine freely. The hydrogen atoms on the disordered dichloromethane molecule were generated geometrically and refined as riding atoms with C−H = 0.95−0.99 Å and $U_{iso}(H) = 1.2U_{eq}(C)$. The maximum and minimum peaks in the final difference Fourier map were +1.705 and −1.619 e·Å^{-3}. This residual density lies very close to the bromine atoms and possibly corresponds to slight bromine disorder. Additional information is given in Table 1 and in the cif file included as Supporting Information.

All DFT calculations were carried out with the BP86[8,9] exchange−correlation functional, augmented with Grimme's dispersion corrections D,[10] STO-TZP basis sets, and a suitably fine grid for numerical integration of matrix elements and tight
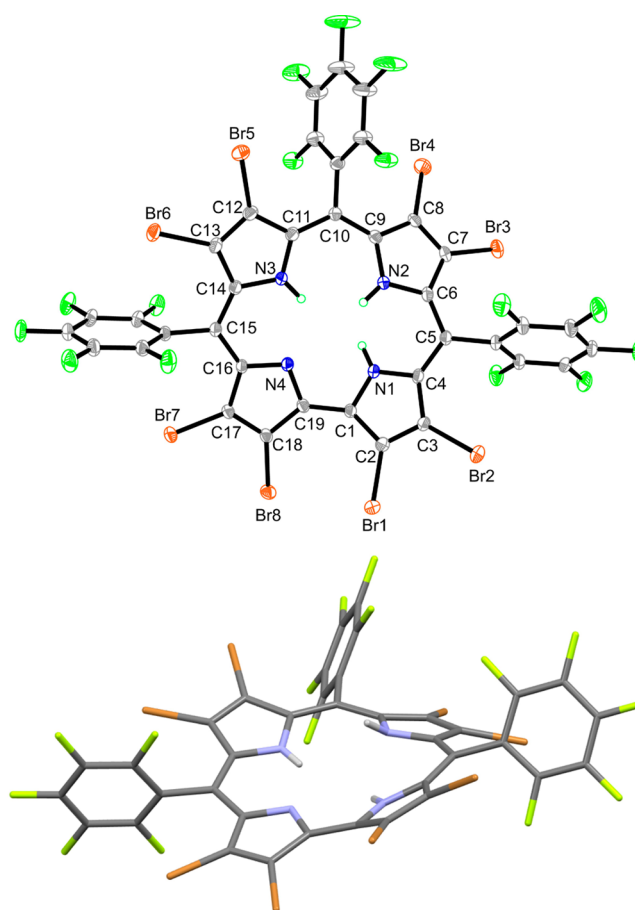
Figure 4. Two views of the X-ray structure of $H_3[Br_8TPFPC]$: thermal ellipsoid plot (top) and wireframe side view (bottom).

convergence criteria for both SCF and geometry iterations, as implemented in the ADF program system.[11] Selected structures and potential energy curves were also calculated with the OLYP and B3LYP functionals, with no significant differences relative to BP86.

■ RESULTS AND DISCUSSION

Figure 2 presents highlights of the BP86-D/TZP optimized geometries of the two tautomers of unsubstituted free-base corrole. Figure 3 presents similar data for the *meso*-triarylcorroles $H_3[TPCor]$ and $H_3[TPFPCor]$, as well as corresponding experimental data derived from X-ray crystal structures. For all free-base corroles examined, the two tautomers were found to be

DFT (Tautomer 1)   DFT (Tautomer 2)

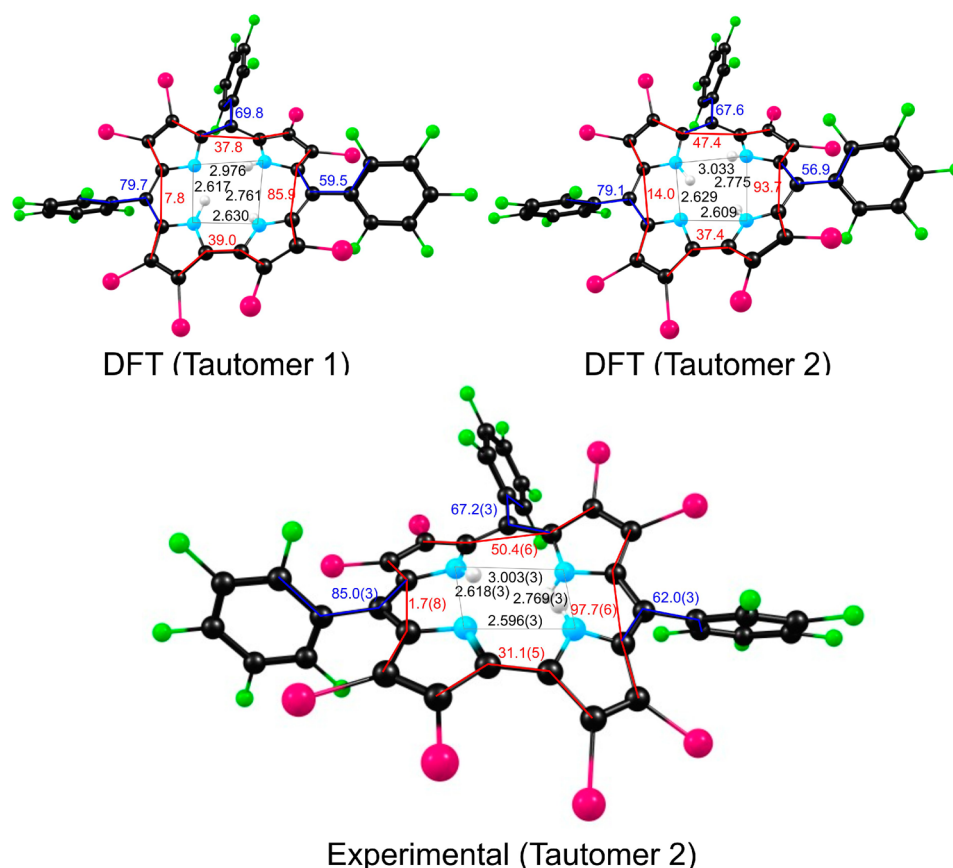Experimental (Tautomer 2)

Figure 5. Experimental and BP86-D/TZP optimized H$_3$[Br$_8$TPFPCor]. Distances (Å) are shown in black, corrole saddling dihedrals in red (deg), and corrole−aryl dihedrals (deg), in blue. Color code of atoms: C (black), N (blue), H (white), F (green), Br (red).
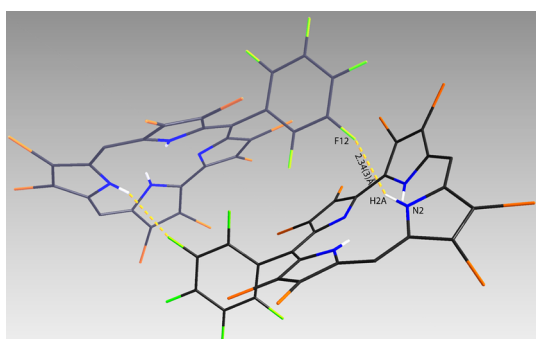

Figure 6. N−H···F−C hydrogen bonding interactions in solid H$_3$[Br$_8$TPFPCor].

almost perfectly equienergetic, i.e., to within 0.05 eV, with a low barrier (0.2 eV) for interconversion. Table 2 lists the so-called "saddling dihedrals" for the various optimized structures. As far as nonplanar distortions are concerned, the main lesson from these results is that, regardless of the tautomeric structure, the saddling dihedral (χ_1) involving pyrrole rings A and B is the highest (>55°), provided the nitrogens in both rings are protonated. The other saddling dihedrals are generally much smaller. A comparison of Figures 2 and 3 also indicates that the free-base *meso*-triarylcorroles exhibit somewhat higher saddling dihedrals than the as yet experimentally unknown parent corrole.

The experimental molecular structure of tautomer 2 of H$_3$(Br$_8$TPFPCor) is extremely distorted (Figures 4 and 5). The χ_1 dihedral is 97.7°, the highest for the nearly 22 or so high-resolution free-base corrole structures reported to date. In other
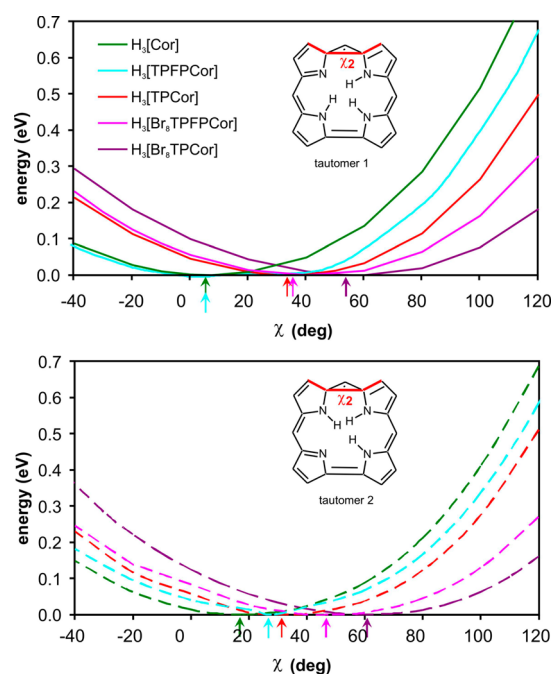

Figure 7. Saddling PE curves as a function of the dihedral indicated (calculated with BP86-D). The solid (top graph) and dotted (bottom graph) lines give the curves for tautomers 1 and 2, respectively. Arrows indicate the minima of the different curves.

words, pyrrole rings A and B are essentially orthogonal to each other, a remarkable distortion for an aromatic compound.

Table 3. Saddling Dihedrals in X-ray Structures of Free-Base Corroles

compound	tautomer	χ_1	χ_2	χ_3	χ_4	CSD	ref
5,5′,10,10′,15,15′-hexakis(pentafluorophenyl)-3,3′-bicorrole, 1,4-dioxane and *n*-octane solvate (dimer)	1	61.8	6.1	21.3	29.8	BATKUE	13
	1	68.8	11.6	21.3	25.8		
2-(4,4,5,5-tetramethyl-(1,3,2)-dioxaborolan-2-yl)-5,10,15-tris(pentafluorophenyl)corrole	1	64.8	10.4	37.5	22.6	CAYZUY	14
5,15-bis(trifluoromethyl)-10-(pentafluorophenyl)corrole	1	64.1	21.7	22.1	14.1	GIBXOF	15
5,10,15-tris(pentafluorophenyl)corrole, ethyl acetate solvate	1	71.0	2.5	44.6	15.3	JEFBIG	11
5,15-bis(pentafluorophenyl)-10-(3-vinylphenyl)corrole	1	59.7	36.8	27.5	11.9	KUHWOA	16
2,3,17-tribromo-5,10,15-tris(pentafluorophenyl)corrole	1	2.3	20.5	73.6	23.4	MULNUD	17
5,10,15-tris(pentafluorophenyl)corrole, chloroform solvate	1	67.8	14.1	28.3	21.1	UCUPOZ	18
5,10,15-tris(perfluorophenyl)corrole, *m*-xylene solvate	1	67.3	14.6	20.0	19.1	UHEWOT	19
10-(4-(5-carboxy-2,7-di-*tert*-butyl-9,9-dimethylxanthyl))-5,15-bis(pentafluorophenyl)corrole, *n*-hexane solvate	1	71.6	20.2	24.1	24.4	UWOCEP	20
5,15-bis(pentafluorophenyl)-10-(2-thienyl)corrole	1	74.4	40.6	8.2	18.1	VAJMAW	21
5,10,15-tris(2,6-difluorophenyl)corrole	1	70.5	15.6	27.4	18.4	XAVBUT	22
5,10,15-triphenylcorrole, methanol solvate	2	55.6	42.0	34.2	20.0	ELAGIH	23
5,10,15-triphenylcorrole	2	77.7	37.5	36.1	5.8	JEFBEC	11
2-bromo-5,10,15-tri-*p*-tolylcorrole, chloroform solvate	2	88.7	26.5	43.1	13.7	MAJMOB	24
18-nitro-5,10,15-tris(4-methylphenyl)corrole, chloroform solvate	2	80.4	34.6	0.3	18.9	QEJPIG	25
5,10,15-tris(heptafluoropropyl)corrole	2	63.6	31.7	15.9	9.8	QORBII	26
10-(4-(5-methoxycarbonyl-2,7-di-*tert*-butyl-9,9-dimethylxanthyl))-5,15-bis(4-*tert*-butylphenyl)corrole, *n*-hexane solvate	2	20.4	6.2	60.8	23.5	UWOCAL	19
3-formyl-5,10,15-triphenylcorrole	2	74.9	30.2	3.5	16.1	XABFIQ	27
5,15-bis(pentafluorophenyl)-10-(4-methoxyphenyl)corrole, *n*-hexane solvate (two molecules in asymmetric unit)	2	74.4	31.5	23.8	13.8	XAVBON	21
	2	73.9	26.7	7.8	20.9		

As shown in Figure 6, the NH unit in ring B engages in hydrogen bonding with a meta-F of a pentafluorophenyl group of an adjacent corrole molecule. Such intermolecular hydrogen bonding has been commonly observed for free-base corroles.

An obvious question concerns to what extent the remarkable distortion of the χ_1 dihedral can be attributed to steric effects of the peripheral substituents. To answer this question, as well as to obtain a general idea of the energetics of nonplanar distortion of free-base corroles, we carried out potential energy scans as a function of the various saddling dihedrals for both tautomers of five corroles: $H_3[Cor]$, $H_3[TPCor]$, $H_3[TPFPCor]$, $H_3[Br_8TPCor]$, and $H_3[Br_8TPFPCor]$. Figure 7 depicts the potential energy curve associated with the saddling dihedral χ_2. On the basis of these results, we are led to conclude that, regardless of the specific system, distortions of ±20° of the dihedrals χ_1 or χ_2 relative to their equilibrium values cost only about 0.05 eV or 1 kcal/mol. Indeed, according to Table 2, the optimized saddling dihedrals of the sterically unhindered corrole $H_3[TPCor]$ are not particularly different from that of $H_3[Br_8TPFPCor]$. A literature survey of saddling dihedrals in free-base corrole structures (where the tautomeric form is clearly assignable), summarized in Table 3, also revealed a handful of sterically unhindered free-base corroles with nonplanar distortions just slightly lower than that observed for $H_3[Br_8TPFPCor]$ in this study.

An intriguing topological property of corrole tautomers is their chirality. Given the strong nonplanar distortions exhibited by some of them, an interesting point concerns the energetics of enantiomerization, which we investigated via a series of constrained geometry optimizations as a function of the dihedral χ'_1 shown in Figure 8. For tautomer 2 of $H_3[Br_8TPFPCor]$, the equilibrium value of this dihedral is approximately 31° and only when the value has reached nearly −26° does the ring system suddenly "invert" and become the other enantiomer. Although a true transition state could not be optimized for this process (a somewhat challenging exercise in view of the size of the system), an activation barrier of about 0.67 eV (15 kcal/mol) may be inferred from Figure 8. A barrier of this magnitude is consistent
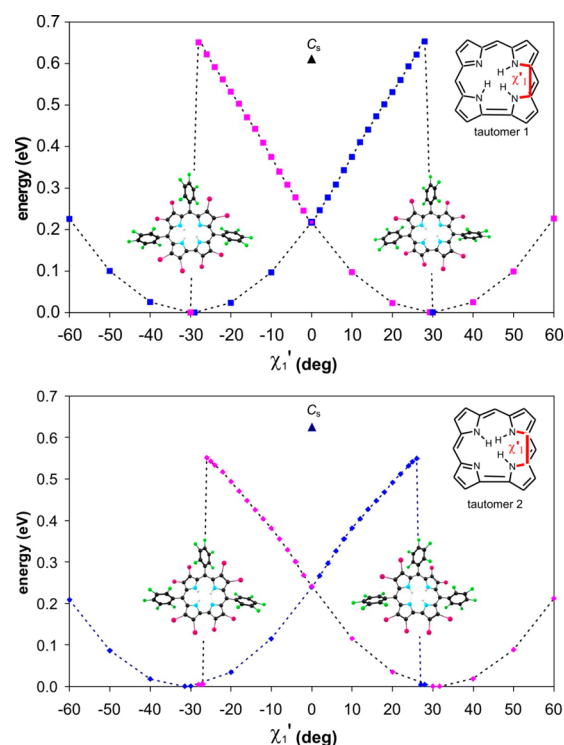

Figure 8. Potential energy curves for tautomers 1 and 2 of $H_3[Br_8TPFPCor]$ as a function of the dihedral indicated (calculated with BP86-D), with all other internal coordinates optimized. Note the abrupt drop in energy at χ'_1 approximately equal to ±28° (0.65 eV) for tautomer 1 and ±26° (0.55 eV) for tautomer 2. The energy of a planar C_s conformation (0.61 eV for tautomer 1 and 0.63 eV for tautomer 2) is indicated by a black triangle.

with the potential isolation, such as via cocrystallization with an enantiopure chiral additive, of a given enantiomer of a free-base corrole.

CONCLUSIONS

The molecular structures of free-base corroles are determined by a complex interplay of aromaticity, steric interactions between multiple NH hydrogens within a congested central cavity, the effects of peripheral substituents, and both intra- and intermolecular hydrogen bonding. Against this backdrop, an X-ray structure of the important ligand 2,3,7,8,12,13,17,18-octabromo-5,10,15-tris(pentafluorophenyl)corrole, $H_3[Br_8TPFPCor]$, corresponding to a specific tautomer, has been found to exhibit the strongest nonplanar distortions observed to date for any free-base corrole. Two adjacent N-protonated pyrrole rings are tilted with respect to each other by approximately 97.7°, whereas the remainder of the molecule is comparatively planar. Interestingly, both X-ray structural data and DFT calculations indicate that the nonplanar distortions of certain sterically unhindered free-base triarylcorroles are only slightly less pronounced than those observed for $H_3[Br_8TPFPCor]$. Steric repulsion among the internal NH hydrogens thus appears to provide the key driving force for nonplanar distortions of meso-triarylcorroles; the presence of additional β-substituents adds marginally to this impetus.

ASSOCIATED CONTENT

Ⓢ Supporting Information

Optimized Cartesian coordinates obtained from DFT calculations. CIF file. This material is available free of charge via the Internet at http://pubs.acs.org.

AUTHOR INFORMATION

Corresponding Author

*A. Ghosh. E-mail: abhik@chem.uit.no.

Notes

The authors declare no competing financial interest.

ACKNOWLEDGMENTS

REFERENCES

(1) Palmer, J. H. Transition Metal Corrole Coordination Chemistry. In *Molecular Electronic Structures of Transition Metal Complexes I. Structure and Bonding. No.142*; Springer-Verlag: Berlin, Heidelberg, 2012; pp 49−89.

(2) Thomas, K. E.; Conradie, J.; Hansen, L.-K.; Ghosh, A. Corroles Cannot Ruffle. *Inorg. Chem.* **2011**, *50*, 3247−3251.

(3) Thomas, K. E.; Conradie, J.; Hansen, L.-K.; Ghosh, A. A Metallocorrole with Orthogonal Pyrrole Rings. *Eur. J. Inorg. Chem.* **2011**, *12*, 1865−1870.

(4) Thomas, K. E.; Alemayehu, A. B.; Conradie, J.; Beavers, C. M.; Ghosh, A. Synthesis and Molecular Structure of Gold Triarylcorroles. *Inorg. Chem.* **2011**, *50*, 12844−12851.

(5) Thomas, K. E.; Alemayehu, A. B.; Conradie, J.; Beavers, C. M.; Ghosh, A. The Structural Chemistry of Metallocorroles: Combined X-ray Crystallography and Quantum Chemistry Studies Afford Unique Insights. *Acc. Chem. Res.* **2012**, *45*, 1203−1214.

(6) Gao, D.; Canard, G.; Giorgi, M.; Balaban, S. *Eur. J. Inorg. Chem.* **2012**, 5915−5920.

(7) Capar, C.; Hansen, L.-K.; Conradie, J.; Ghosh, A. β-Octabromo-meso-tris(pentafluorophenyl)corrole: Reductive Demetalation-Based Synthesis of a Heretofore Inaccessible, Perhalogenated Free-Base Corrole. *J. Porphyrins Phthalocyanines* **2010**, *14*, 509−512.

(8) Becke, A. D. Density-Functional Exchange-Energy Approximation with Correct Asymptotic Behaviour. *Phys. Rev.* **1988**, *A38*, 3098−3100.

(9) Perdew, J. P. Density-Functional Approximation for the Correlation Energy of the Inhomogeneous Electron Gas. *Phys. Rev.* **1986**, *B33*, 8822−8824. Erratum: Perdew, J. P. *Phys. Rev.* **1986**, *B34*, 7406.

(10) Grimme, S. Semiempirical GGA-Type Density Functional Constructed with a Long-Range Dispersion Correction. *J. Comput. Chem.* **2006**, *27*, 1787−1799.

(11) Van Gisbergen, S. J. A. Amsterdam Density Functional Molecular Modelling Suite. May be obtained from: Scientific Computing & Modelling NV, Division of Theoretical Chemistry, Vrije Universiteit, De Boelelaan 1083, Amsterdam 1081 HV, The Netherlands, www.scm.com.

(12) Ding, T.; Harvey, J. D.; Ziegler, C. J. N-H Tautomerization in Triaryl Corroles. *J. Porphyrins Phthalocyanines* **2005**, *9*, 22−27.

(13) Hirabayashi, S.; Omote, M.; Aratani, N.; Osuka, A. Directly Linked Corrole Oligomers via Facile Oxidative 3−3′ Coupling Reaction. *Bull. Chem. Soc. Jpn.* **2012**, *85*, 558−562.

(14) Hiroto, S.; Hisaki, I.; Shinokubo, H.; Osuka, A. Synthesis of Corrole Derivatives through Regioselective Ir-Catalyzed Direct Borylation. *Angew. Chem., Int. Ed.* **2005**, *44*, 6763−6766.

(15) Goldschmidt, R.; Goldberg, I.; Balazs, Y.; Gross, Z. Synthesis and Properties of a Corrole with Small and Electron-Withdrawing Substitutents, 5,15-Bis(trifluoromethyl)-10-pentafluorophenylcorrole. *J. Porphyrins Phthalocyanines* **2006**, *10*, 76−86.

(16) Kim, K.; Kim, I.; Maiti, N.; Kwon, S. J.; Bucella, D.; Egorova, O. A.; Lee, Y. S.; Kwak, J.; Churchill, D. G. A Study of Nerve Agent Model Organophosphonate Binding with Manganese-A₂B-Corrole and -A₂B₂-Porphyrin Systems. *Polyhedron* **2009**, *28*, 2418−2430.

(17) Du, R.-B.; Liu, C.; Shen, D.-M.; Chen, Q.-Y. Partial Bromination and Fluoroalkylation of 5,10,15-Tris(pentafluorophenyl)corrole. *Synlett.* **2009**, 2701−2705.

(18) Reith, L. M.; Stiftinger, M.; Monkowius, U.; Knör, G.; Schöfberger, W. Synthesis and Characterization of a Stable Bismuth(III) A₃−Corrole. *Inorg. Chem.* **2011**, *50*, 6788−6797.

(19) Gross, Z.; Galili, N.; Simkhovich, L.; Saltsman, I.; Botoshansky, M.; Blaser, D.; Boese, R.; Goldberg, I. Solvent-Free Condensation of Pyrrole and Pentafluorobenzaldehyde: A Novel Synthetic Pathway to Corrole and Oligopyrromethenes. *Org. Lett.* **1999**, *1*, 599−602.

(20) Dogutan, D. K.; Stoian, S. A.; McGuire, R., Jr.; Schwalbe, M.; Teets, T. S.; Nocera, D. G. Hangman Corroles: Efficient Synthesis and Oxygen Reaction Chemistry. *J. Am. Chem. Soc.* **2011**, *133*, 131−140.

(21) Egorova, O. A.; Tsay, O. G.; Khatua, S.; Meka, B.; Maiti, N.; Kim, M.-K.; Kwon, S. J.; Huh, J. O.; Bucella, D.; Kang, S.-O.; et al. Synthetic, Cyclic Voltammetric, Structural, EPR, and UV−Vis Spectroscopic Studies of Thienyl-Containing meso-A₂B-cor(Cr^V=O) Systems: Consideration of Three Interrelated Molecular Detection Modalities. *Inorg. Chem.* **2010**, *49*, 502−512.

(22) Kumar, A.; Goldberg, I.; Botoshansky, M.; Buchman, Y.; Gross, Z. Oxygen Atom Transfer Reactions from Isolated (Oxo)manganese(V) Corroles to Sulfides. *J. Am. Chem. Soc.* **2010**, *132*, 15233−15245.

(23) Paolesse, R.; Marini, A.; Nardis, S.; Froiio, A.; Mandoj, F.; Nurco, D. J.; Prodi, L.; Montalti, M.; Smith, K. M. Novel Routes to Substituted 5,10,15-Triarylcorroles. *J. Porphyrins Phthalocyanines* **2003**, *7*, 25−36.

(24) Nardis, S.; Pomarico, G.; Mandoj, F.; Fronczek, F. R.; Smith, K. M.; Paolesse, R. One-Pot Synthesis of Meso-Alkyl Substituted Isocorroles: The Reaction of a Triarylcorrole with Grignard Reagent. *J. Porphyrins Phthalocyanines* **2010**, *14*, 752−758.

(25) Stefanelli, M.; Pomarico, G.; Tortora, L.; Nardis, S.; Fronczek, F. R.; McCandless, G. T.; Smith, K. M.; Manowong, M.; Fang, Y.; Chen, P.; et al. β-Nitro-5,10,15-tritolylcorroles. *Inorg. Chem.* **2012**, *51*, 6928−6942.

(26) Simkhovich, L.; Goldberg, I.; Gross, Z. First Syntheses and X-ray Structures of a Meso-alkyl Substituted Corrole and its Ga(III) Complex. *J. Inorg. Biochem.* **2000**, *80*, 235−238.

(27) Paolesse, R.; Nardis, S.; Venanzi, M.; Mastroianni, M.; Russo, M.; Fronczek, F. R.; Vicente, M. G. H. Vilsmeier Formylation of 5,10,15-Triphenylcorrole: Expected and Unusual Products. *Chem. Eur. J.* **2003**, *9*, 1192−1197.